

# Comparison of superconducting pairing in doped cuprates and nickelates within an extended Hubbard model

Yicheng Xiong,<sup>1</sup> Hang Ma,<sup>1</sup> Hongxing Liu,<sup>1</sup> Runyu Ma,<sup>1</sup> and Tianxing Ma<sup>1,2,\*</sup>

<sup>1</sup>*School of Physics and Astronomy, Beijing Normal University, Beijing 100875, China*

<sup>2</sup>*Key Laboratory of Multiscale Spin Physics (Ministry of Education),  
Beijing Normal University, Beijing 100875, China*

Within an extended Hubbard model, we investigate the superconducting pairing behavior of infinite-layer nickelate NdNiO<sub>2</sub> and cuprates superconductors by using the determinant quantum Monte Carlo method. Our focus is on comparing their dominant pairing symmetries. The results indicate that the  $d_{x^2-y^2}$  pairing interaction is significantly enhanced at low temperatures in both doped nickelates and cuprates, while other typical pairing symmetries are effectively suppressed, highlighting the dominance of  $d_{x^2-y^2}$  pairing form. Additionally, we find that the effective pairing interaction for  $d_{x^2-y^2}$  pairing in doped nickelates is slightly lower than that in doped cuprates, which may be attributed to the different degrees of Fermi surface warping caused by the third nearest hopping  $t''$ . Further studies show that the hole doping and interaction strength have significant effects on the  $d_{x^2-y^2}$  pairing interaction within the selected parameter range. The  $d_{x^2-y^2}$  pairing interaction is notably weakened when the hole doping increases, while it is significantly enhanced with increasing Coulomb interaction strength  $U$ . This comparative analysis reveals the similarities and differences in the pairing behaviors of doped nickelates and cuprates, which may provide further insights into understanding the superconducting properties of these two classes of materials.

## I. INTRODUCTION

Since the discovery of high- $T_c$  superconductivity in doped cuprates<sup>1</sup>, unraveling the mechanism of superconductivity<sup>2-6</sup> and the dependence of the transition temperature on material properties have been central issues in condensed matter physics. Comparative studies of materials with similar features but different chemical compositions should be an effective way to understand this problem. Recent breakthroughs in nickelates, such as the achievement of superconducting transition temperatures up to 15 K in Nd<sub>1-x</sub>Sr<sub>x</sub>NiO<sub>2</sub><sup>7,8</sup> and 9 K in La<sub>1-x</sub>Sr<sub>x</sub>NiO<sub>2</sub><sup>9</sup>, have provided new perspectives for understanding the pairing mechanism in high-temperature superconductors. The  $3d^9$  electronic configuration of Ni<sup>+</sup> in NdNiO<sub>2</sub> resembles that of Cu<sup>2+</sup> in cuprates<sup>10,11</sup>. The Ni<sup>+</sup> oxidation state is stabilized in the infinite-layer square-planar RNiO<sub>2</sub> ( $R = \text{La, Nd, Pr}$ )<sup>12,13</sup>, which possesses the same P4/mmm crystal structure as the parent compounds of high- $T_c$  cuprates<sup>14</sup>. Superconductivity is also observed when substituting neodymium with other lanthanides<sup>9,13,15</sup> and in more complex multilayer structures<sup>16</sup>. These findings reveal an intrinsic similarity between doped nickelates and cuprates.

Recently, various experimental studies<sup>13,17-23</sup> and theoretical approaches, including dynamical mean-field theory (DMFT)<sup>24-26</sup>, density functional theory (DFT)<sup>25,27-31</sup>, and model studies<sup>28,32-34</sup>, have been employed to investigate the essential low-energy physics of doped nickelates and its similarities and differences with that of doped cuprates. First-principles calculations based on DFT suggest that the electron-phonon coupling is insufficient to account for the superconducting transition temperature up to 15 K<sup>35</sup>, and the superconductivity is more likely driven by

electron-electron interactions. Furthermore, recent studies have revealed a dome-shaped dependence of the superconducting  $T_c$  on the doping<sup>3,36</sup>, akin to the behavior of doped cuprates.

Another key question worth exploring is whether the unique physical phenomena observed in these materials can be fundamentally explained by the single-band model. In doped nickelates and cuprates, the low-energy degrees of freedom are predominantly determined by the  $3d$  orbitals. However, their electronic structures exhibit some differences. First, unlike doped cuprates, the energy difference between O- $2p$  and Ni- $3d$  in doped nickelates is much larger than the Coulomb interaction between Ni- $3d$  electrons<sup>34,37-39</sup>, leading to the direct entry of additional holes into Ni- $3d$  orbitals rather than the formation of Zhang-Rice singlets<sup>28</sup>. Therefore, the influence of O- $2p$  degree of freedom can be safely neglected. Second, the electron pockets contributed by the  $R$ - $5d$  ( $R = \text{Nd, La}$ ) degrees of freedom in the parent compounds occupy a small part of the Brillouin zone<sup>40</sup>, having a minor impact on the low-energy physics in the hole-doped case and can be neglected<sup>29,31,35,41</sup>. Furthermore, DMFT calculations indicate that in Sr-doped NdNiO<sub>2</sub> superconductors with Sr doping not exceeding 30%, holes primarily reduce the occupancy of the Ni- $3d_{x^2-y^2}$  and Nd- $5d$  bands<sup>42,43</sup>, essentially rendering the system as a single Ni- $3d_{x^2-y^2}$  orbital. Therefore, given consideration of electronic correlation effects, the single-band Hubbard model is sufficient to capture the low-energy physical properties of NdNiO<sub>2</sub> within an appropriate doping range.

Determining the dominant superconducting pairing symmetry remains a crucial research objective and a major challenge in the field. Previous single-orbital<sup>34,43,44</sup>, and multi-orbital studies<sup>40,45,46</sup> have yielded different conclusions regarding the dominant

arXiv:2406.08717v1 [cond-mat.str-el] 13 Jun 2024

pairing symmetry. By using the determinant quantum Monte Carlo (DQMC) method, we systematically investigate the superconducting pairing properties of the infinite-layer nickelate  $\text{NdNiO}_2$  and typical cuprate superconductors under the single-band Hubbard model. We find that at low temperatures, the  $d_{x^2-y^2}$  pairing symmetry is significantly enhanced while other typical pairing symmetries are effectively suppressed within the given doping range, indicating the dominance of  $d_{x^2-y^2}$  pairing. The interaction strength  $U$  ratio to nearest hopping  $U/t$ , as well as the relative strength of long-range hopping to nearest hopping in the single-band model<sup>47</sup>, are important factors. With increasing Coulomb interaction strength  $U$ , the pairing susceptibility of the  $d_{x^2-y^2}$  channel is significantly enhanced, indicating that electronic correlations play a crucial role in promoting  $d_{x^2-y^2}$  pairing. Furthermore, we find that the third nearest hopping  $t''$  has a certain suppressive effect on the  $d_{x^2-y^2}$  pairing channel.

## II. MODEL AND METHODS

In the single-band Hubbard model, the nickel-square lattice Hamiltonian can be written as

$$H = H_K + H_\mu + H_V, \quad (1)$$

$$H_K = -t \sum_{\langle i,j \rangle, \sigma} (c_{i\sigma}^\dagger c_{j\sigma} + c_{j\sigma}^\dagger c_{i\sigma}) \\ - t' \sum_{\langle i,j \rangle, \sigma} (c_{i\sigma}^\dagger c_{j\sigma} + c_{j\sigma}^\dagger c_{i\sigma}) \\ - t'' \sum_{\langle i,j \rangle, \sigma} (c_{i\sigma}^\dagger c_{j\sigma} + c_{j\sigma}^\dagger c_{i\sigma}), \quad (2)$$

$$H_\mu = -\mu \sum_{\mathbf{i}} (n_{i\uparrow} + n_{i\downarrow}), \quad (3)$$

$$H_V = U \sum_{\mathbf{i}} (n_{i\uparrow} - \frac{1}{2})(n_{i\downarrow} - \frac{1}{2}). \quad (4)$$

For the copper-oxygen plane, we take the nearest hopping  $t$  as the unit of energy (set to 1), the second nearest hopping  $t' = -0.25t$ , and the third nearest hopping  $t'' = 0$ . For the nickel-oxygen plane, we take  $t = 1$ ,  $t' = -0.25t$ , and  $t'' = 0.12t$ . These parameters are derived from DFT<sup>44,48-50</sup>. The fermionic operators  $c_{i\sigma}^\dagger$  and  $c_{i\sigma}$  represent the creation and annihilation of an electron with spin  $\sigma$  ( $\sigma = \uparrow, \downarrow$ ) at site  $i$ , respectively, satisfying the anticommutation relations. The particle number operator  $n_{i\sigma} = c_{i\sigma}^\dagger c_{i\sigma}$  gives the number of electrons with spin  $\sigma$  at site  $i$ . The chemical potential  $\mu$  is used to tune the electron density of the system. By changing the value of  $\mu$ , one can control the doping level of the system.

We employ the DQMC method to simulate the lattice shown in Fig. 1(b) under periodic boundary conditions. This approach maps the interacting fermion model onto a system of free fermions coupled to auxiliary

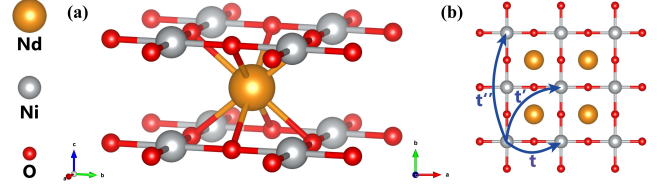


FIG. 1. (Color online) (a) presents the crystal structure of  $\text{NdNiO}_2$  compound, which consists of Nd, Ni, and O atoms, exhibiting a distinct layered arrangement. (b) provides a top view of the lattice structure of  $\text{NdNiO}_2$  compound, where the three blue arrows represent the nearest, second nearest, and third nearest hopping modes of electrons in the lattice, respectively.

fields. By utilizing the Suzuki-Trotter decomposition and Hubbard-Stratonovich (HS) transformation to handle the interaction terms, the partition function  $Z$  contains only quadratic fermion operators, enabling the calculation of the fermion trace. To ensure reliable results, we first perform 8000 Monte Carlo sweeps to thermalize the system, followed by an additional 30000 to 120000 sweeps for statistical averaging of physical quantities, depending on the complexity of the system. We divide the independent measurements into 20 equal-length intervals, perform coarse-grained averaging for each interval, and estimate the uncertainty of the simulation results using the standard deviation of the 20 averages, thereby reducing the statistical fluctuations of physical quantities. For more technical details regarding DQMC method, please refer to the relevant literature<sup>51-55</sup>.

To investigate the superconductivity in doped nickelates and cuprates, we define the superconducting pairing susceptibility as

$$P_\alpha = \frac{1}{N_s} \sum_{\mathbf{i}, \mathbf{j}} \int_0^\beta d\tau \langle \Delta_\alpha^\dagger(\mathbf{i}, \tau) \Delta_\alpha(\mathbf{j}, 0) \rangle, \quad (5)$$

where the superconducting order parameter  $\Delta_\alpha^\dagger(\mathbf{i})$  is given by

$$\Delta_\alpha^\dagger(\mathbf{i}) = \sum_l f_\alpha^\dagger(\delta_l) (c_{i\uparrow} c_{i+\delta_l\downarrow} - c_{i\downarrow} c_{i+\delta_l\uparrow})^\dagger \quad (6)$$

The phase factors  $\delta_l$  associated with different pairing forms determine superconducting pairing symmetry  $\alpha$ . In the square lattice, we investigate the pairing forms shown in Fig. 2(a)-(d). The structure factors of these pairing symmetries can be expressed as follows:

$$\begin{aligned} s\text{-wave} : f_s(\delta_l) &= 1(\delta_l = (\pm x, \pm \hat{y})), \\ d_{x^2-y^2}\text{-wave} : f_{d_{x^2-y^2}}(\delta_l) &= 1(\delta_l = (\pm \hat{x}, 0)), \\ &\text{and } f_{d_{x^2-y^2}}(\delta_l) = -1(\delta_l = (0, \pm \hat{y})), \\ s_{xy}\text{-wave} : f_{s_{xy}}(\delta_l) &= 1(\delta_l = \pm(x, \pm \hat{y})), \\ d_{xy}\text{-wave} : f_{d_{xy}}(\delta_l) &= 1(\delta_l = \pm(-\hat{x}, \hat{y})), \\ &\text{and } f_{d_{xy}}(\delta_l) = -1(\delta_l = \pm(\hat{x}, \hat{y})). \end{aligned} \quad (7)$$

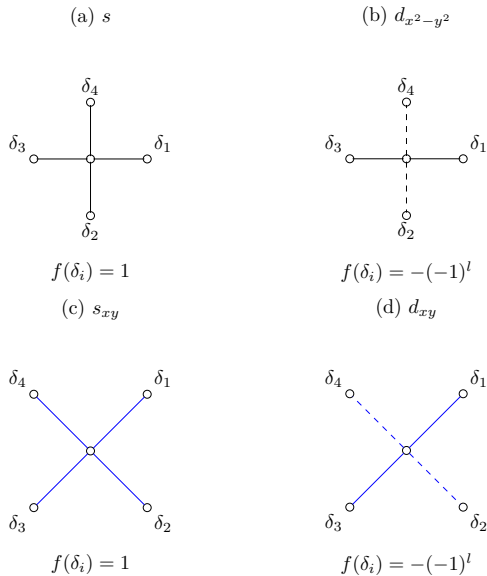


FIG. 2. (Color online) The five pairing forms possess different symmetries and phases. Specifically, (a) is the  $s$ -wave, (b) is the  $d_{x^2-y^2}$ -wave, (c) is the  $s_{xy}$ -wave, (d) is the  $d_{xy}$ -wave

To determine the dominant pairing symmetry in doped nickelates and cuprates, we introduce the effective pairing interaction  $\bar{P}\alpha = P\alpha - \tilde{P}\alpha$ <sup>54,56–58</sup>, where the uncorrelated single-particle contribution  $\tilde{P}\alpha$  can be obtained by replacing  $\langle c_{i\downarrow}^\dagger c_{j\downarrow} c_{i+\delta_{l'}}^\dagger c_{j+\delta_{l'}} \rangle$  with  $\langle c_{i\downarrow}^\dagger c_{j\downarrow} \rangle \langle c_{i+\delta_{l'}}^\dagger c_{j+\delta_{l'}} \rangle$  in Eq. (6). A positive effective pairing interaction indicates that the superconducting pairing form is driven by electron-electron correlations, whereas a negative value suggests that this superconducting pairing channel may be suppressed by other pairing channels.

### III. RESULTS

Our main simulations are performed on a two-dimensional square lattice with  $8 \times 8$  sites, and further results are also checked on a lattice with  $12 \times 12$  sites, which is fair large for DQMC method. We investigated the temperature dependence of the effective pairing interactions for various candidate pairing symmetries with these lattices. As shown in Fig. 3, at low temperatures, we observed a significant enhancement in the effective pairing interaction of the  $d_{x^2-y^2}$  symmetry in both doped nickelates and cuprates. This suggests that the  $d_{x^2-y^2}$  pairing symmetry may play a crucial role in these strongly correlated electron systems. However, it is noteworthy that the  $d_{x^2-y^2}$  effective pairing interaction in doped nickelates is slightly lower in magnitude compared to that of doped cuprates. This discrepancy may be attributed to different degrees of Fermi surface warping caused by distinct tight-binding

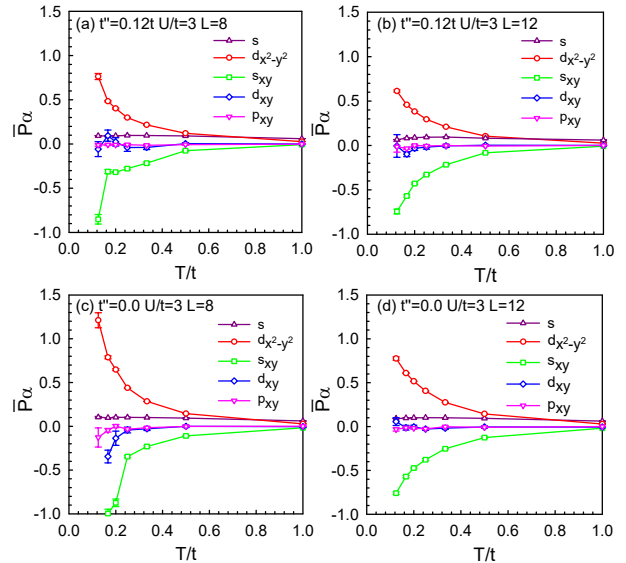


FIG. 3. (Color online) (a) and (b) show the temperature dependence of the effective pairing interaction for different candidate pairing symmetries in doped nickelate with lattice sizes of  $8 \times 8$  and  $12 \times 12$ , respectively, at  $U/t = 3$  and electron density  $\langle n \rangle = 0.8$ . (c) and (d) present the corresponding results for doped cuprates under the same conditions.

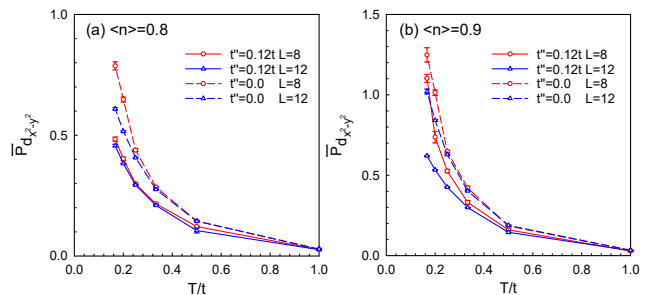


FIG. 4. (Color online) Temperature dependence of the effective  $d_{x^2-y^2}$  pairing interaction for doped nickelates (solid lines) and cuprates (dashed lines) at different lattice sizes, where circles represent  $L = 8$  and upward triangles represent  $L = 12$ . The calculations are performed with  $U/t = 3$  and the electron density  $\langle n \rangle = 0.8, 0.9$ .

parameters. Meanwhile, we examined other typical superconducting pairing symmetries, namely  $s$ -wave,  $s_{xy}$ -wave,  $d_{xy}$ -wave, and  $p_{xy}$ -wave. The results indicate that the effective pairing interactions for these channels are either close to zero or negative. This implies that the  $d_{x^2-y^2}$  superconducting pairing symmetry has an intrinsic competitive advantage over other pairing channels, effectively suppressing the formation of other superconducting states. This finding provides strong evidence for the dominance of  $d_{x^2-y^2}$  pairing symmetry near optimal doping.

We also investigated the influence of lattice size on the computational results. As shown in Fig. 4, the  $d_{x^2-y^2}$

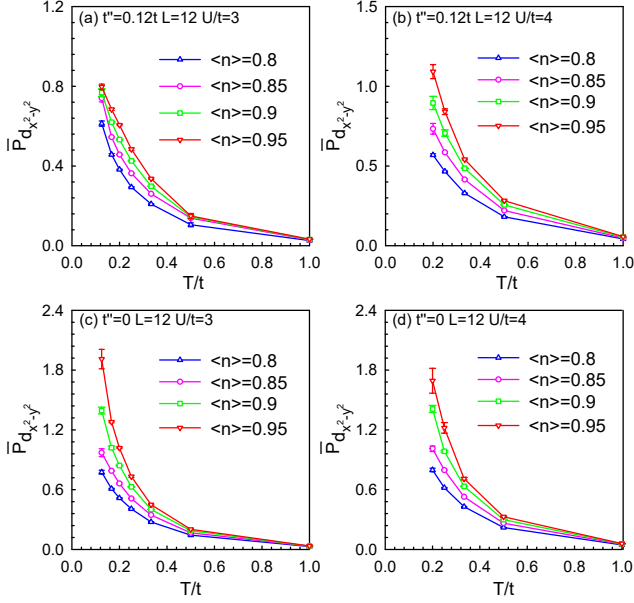


FIG. 5. (Color online) Temperature dependence of the effective  $d_{x^2-y^2}$  pairing interaction for doped nickelates and cuprates at different hole doping. (a) and (b) show the results for doped nickelates with lattice size  $L = 12$  and Coulomb interaction strength  $U/t = 3$  and  $4$ , respectively. (c) and (d) present the corresponding results for doped cuprates under the same conditions.

pairing channel exhibits a weak dependence on lattice size in both doped cuprates and nickelates. The effective pairing interaction remains nearly constant with varying lattice size, indicating the robustness of the  $d_{x^2-y^2}$  wave dominance.

To systematically investigate the influence of hole doping on the temperature dependence of the  $d_{x^2-y^2}$  effective pairing interaction, in Fig. 5, we presents the evolution of the  $d_{x^2-y^2}$  effective pairing interaction as a function of temperature for doped cuprate and nickelate compounds at  $U/t = 3, 4$  and electron filling  $\langle n \rangle = 0.8, 0.85, 0.9, 0.95$ . Within the studied parameter range, as the electron filling gradually deviates from half-filling, the  $d_{x^2-y^2}$  effective pairing interaction exhibits a significant decreasing trend in both materials, especially more pronounced in the low-temperature region. This indicates that the superconducting pairing has a strong dependence on electron filling, which is a common feature of doped cuprates and nickelates. This may originate from the strong Coulomb repulsion between  $d$ -orbital electrons in the  $\text{CuO}_2$  and  $\text{NiO}_2$  planes, leading to the formation of a Mott insulating state near half-filling. Moderate hole or electron doping can destroy the Mott insulating state, introduce charge carriers, and thus realize high-temperature superconductivity.

Figs. 6 and 7 clearly demonstrate the impact of the Coulomb interaction strength  $U$  on the effective pairing interaction  $\bar{P}_{d_{x^2-y^2}}$  in the  $d_{x^2-y^2}$  pairing channel for doped nickelates and cuprates. As  $U$  gradually

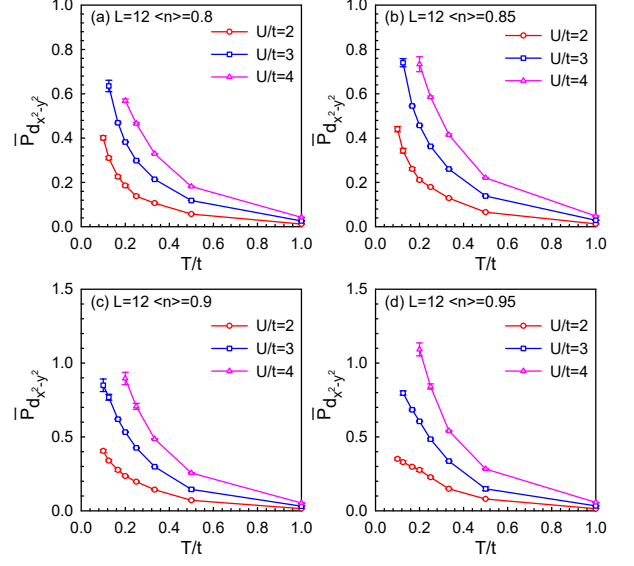


FIG. 6. (Color online) Temperature dependence of the  $d_{x^2-y^2}$  effective pairing interaction  $\bar{P}_{d_{x^2-y^2}}$  in doped nickelates at different electron densities  $\langle n \rangle$ : (a)  $\langle n \rangle = 0.8$ , (b)  $\langle n \rangle = 0.85$ , (c)  $\langle n \rangle = 0.9$ , and (d)  $\langle n \rangle = 0.95$ . The curves correspond to various Coulomb interaction strengths  $U$ . The calculations are performed on a lattice size of  $L = 12$ .

increases, the  $\bar{P}_{d_{x^2-y^2}}$  of both materials exhibits a significant enhancement trend, indicating that electronic correlation effects play a crucial role in promoting  $d_{x^2-y^2}$  superconducting pairing. It is noteworthy that in the low-temperature region, the  $\bar{P}_{d_{x^2-y^2}}$  of doped cuprates shows a more pronounced divergence behavior, especially at larger  $U$  values. This divergence trend foreshadows the formation of  $d_{x^2-y^2}$  superconducting pairing. In contrast, the divergence of  $\bar{P}_{d_{x^2-y^2}}$  in doped nickelates at low temperatures is less evident, suggesting that their  $d$ -wave superconducting pairing may not be as stable and prominent as in doped cuprates.

Finally, we investigated the competitive advantage of the  $d_{x^2-y^2}$  wave pairing channel under different  $t''$  values. As shown in Fig. 8(a), when  $U/t = 3$  and  $\langle n \rangle = 0.8, 0.85, 0.9, 0.95$  are fixed, and  $t''$  is increased, the effective pairing interaction of the  $d_{x^2-y^2}$  wave exhibits a weakening effect. Similarly, as shown in Fig. 8(b), when  $\langle n \rangle = 0.8$  and  $U/t = 2, 3, 4$  are fixed, and  $t''$  is increased, the pairing susceptibility of the  $d_{x^2-y^2}$  wave also shows a weakening effect. This indicates that within the selected parameter range,  $t''$  has a certain inhibitory effect on the  $d_{x^2-y^2}$  superconducting pairing channel. This result reveals the important role of the third hopping in regulating the  $d_{x^2-y^2}$  wave superconducting pairing strength for doped nickelates and cuprates. This may be because reducing  $t''$  correspondingly reduces the warping of the Fermi surface. Under optimal parameter conditions, as the Fermi surface flattens, superconductivity is enhanced<sup>44</sup>.

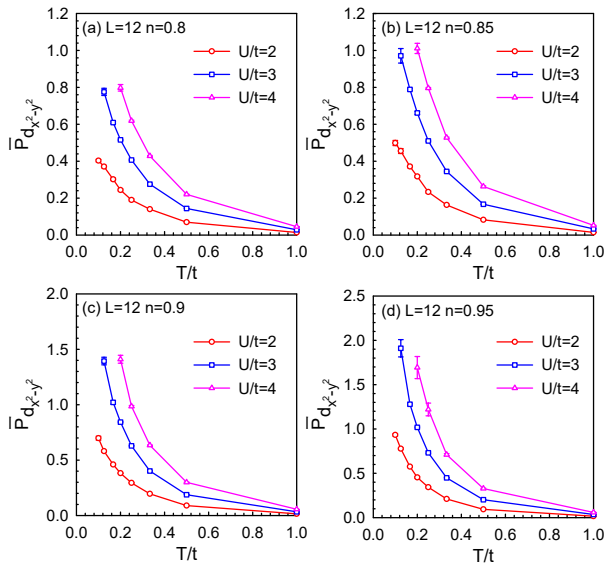


FIG. 7. (Color online) Temperature dependence of the  $d_{x^2-y^2}$  effective pairing interaction  $\bar{P}_{d_{x^2-y^2}}$  in doped cuprates at different electron densities  $\langle n \rangle$ : (a)  $\langle n \rangle = 0.8$ , (b)  $\langle n \rangle = 0.85$ , (c)  $\langle n \rangle = 0.9$ , and (d)  $\langle n \rangle = 0.95$ . The curves correspond to various Coulomb interaction strengths  $U$ . The calculations are performed on a lattice size of  $L = 12$ .

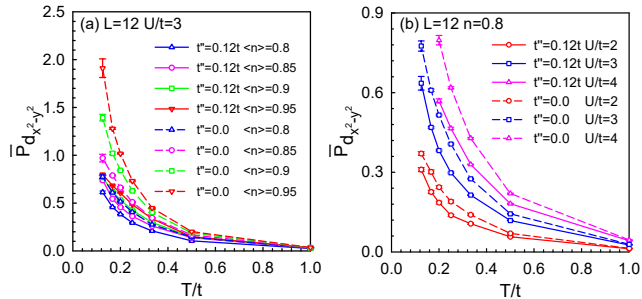


FIG. 8. (Color online) (a) Temperature dependence of the  $d_{x^2-y^2}$ -wave pairing susceptibility  $\bar{P}_{d_{x^2-y^2}}$  for different  $t''$  values at lattice size  $L = 12$ , interaction strength  $U/t = 3$ , and electron densities  $\langle n \rangle = 0.8, 0.85, 0.9, 0.95$ . (b) Temperature dependence of the  $d_{x^2-y^2}$ -wave pairing susceptibility  $P_{d_{x^2-y^2}}$  for different  $t''$  values at lattice size  $L = 12$ , electron density  $\langle n \rangle = 0.8$ , and interaction strengths  $U/t = 2, 3, 4$ .

It is worth noting that although  $t''$  has a certain inhibitory effect on the  $d_{x^2-y^2}$  wave superconducting pairing channel, this effect is not significant in actual nickelates and cuprates. This is because in these materials, the magnitude of  $t''$  is usually much smaller than the nearest hopping  $t$ , and thus its impact on the shape of the Fermi surface is relatively limited. In contrast, the interaction strength  $U$  and the hole doping  $\langle n \rangle$  have a more significant impact on the  $d_{x^2-y^2}$  wave superconducting pairing.

#### IV. SUMMARY

We constructed two-dimensional square lattice models of varying lattice sizes to study the temperature dependence of the effective pairing interactions for different candidate pairing symmetries. The results show that at low temperatures, the  $d_{x^2-y^2}$  pairing symmetry dominates in both doped nickelates and cuprates, with a significant enhancement in the effective pairing interaction, indicating that  $d_{x^2-y^2}$  pairing plays a crucial role in these strongly correlated systems. However, the magnitude of the  $d_{x^2-y^2}$  effective pairing interaction in doped nickelates is slightly smaller than that in doped cuprates, possibly due to differences in their tight-binding parameters, leading to variations in Fermi surface warping. We also investigated the effect of hole doping on the  $d_{x^2-y^2}$  effective pairing interaction. The results indicate that as the filling deviates from half-filling, the  $d_{x^2-y^2}$  effective pairing interaction significantly weakens in the low-temperature region, suggesting a dependence of superconducting pairing on electron filling. Additionally, with increasing Coulomb interaction strength  $U$ , the  $d_{x^2-y^2}$  pairing interaction is significantly enhanced, indicating that electron correlation effects play a key role in promoting  $d_{x^2-y^2}$  superconducting pairing. Finally, we found that the third hopping  $t''$  has a certain inhibitory effect on the  $d_{x^2-y^2}$  wave pairing channel. However, the Coulomb interaction strength  $U$  and hole doping  $\langle n \rangle$  have a more significant impact on  $d_{x^2-y^2}$  wave pairing.

*Acknowledgments* This work was supported by Beijing Natural Science Foundation (No. 1242022), and Guangxi Key Laboratory of Precision Navigation Technology and Application, Guilin University of Electronic Technology (No. DH202322). The numerical simulations in this work were performed at the HSCC of Beijing Normal University.

\* txma@bnu.edu.cn

<sup>1</sup> J. G. Bednorz and K. A. Müller, *Z. Phys. B: Condens. Matter* **64**, 189 (1986).

<sup>2</sup> P. W. Anderson, P. A. Lee, M. Randeria, T. M. Rice, N. Trivedi, and F. C. Zhang, *J. Phys.: Condens. Matter* **16**, R755 (2004).

<sup>3</sup> M. Azuma, Z. Hiroi, M. Takano, Y. Bando, and Y. Takeda, *Nature* **356**, 775 (1992).

<sup>4</sup> A. Damascelli, Z. Hussain, and Z.-X. Shen, *Rev. Mod. Phys.* **75**, 473 (2003).

<sup>5</sup> P. A. Lee, N. Nagaosa, and X.-G. Wen, *Rev. Mod. Phys.* **78**, 17 (2006).

<sup>6</sup> D. J. Scalapino, *Rev. Mod. Phys.* **84**, 1383 (2012).

<sup>7</sup> D. Li, K. Lee, B. Y. Wang, M. Osada, S. Crossley, H. R. Lee, Y. Cui, Y. Hikita, and H. Y. Hwang, *Nature* **572**, 624 (2019).

- <sup>8</sup> G. A. Sawatzky, *Nature* **572**, 592 (2019).
- <sup>9</sup> M. Osada, B. Y. Wang, B. H. Goodge, S. P. Harvey, K. Lee, D. Li, L. F. Kourkoutis, and H. Y. Hwang, *Adv. Mater.* **33**, 2104083 (2021).
- <sup>10</sup> V. I. Anisimov, D. Bukhvalov, and T. M. Rice, *Phys. Rev. B* **59**, 7901 (1999).
- <sup>11</sup> K.-W. Lee and W. E. Pickett, *Phys. Rev. B* **70**, 165109 (2004).
- <sup>12</sup> M. A. Hayward, M. A. Green, M. J. Rosseinsky, and J. Sloan, *J. Am. Chem. Soc.* **121**, 8843 (1999).
- <sup>13</sup> M. Osada, B. Y. Wang, K. Lee, D. Li, and H. Y. Hwang, *Phys. Rev. Mater.* **4**, 121801 (2020).
- <sup>14</sup> A. S. Botana and M. R. Norman, *Phys. Rev. X* **10**, 011024 (2020).
- <sup>15</sup> S. Zeng, C. Li, L. E. Chow, Y. Cao, Z. Zhang, C. S. Tang, X. Yin, Z. S. Lim, J. Hu, P. Yang, and A. Ariando, *Sci. Adv.* **8**, eabl9927 (2022).
- <sup>16</sup> G. A. Pan, D. Ferenc Segedin, H. LaBollita, Q. Song, E. M. Nica, B. H. Goodge, A. T. Pierce, S. Doyle, S. Novakov, D. Córdova Carrizales, A. T. N'Diaye, P. Shafer, H. Paik, J. T. Heron, J. A. Mason, A. Yacoby, L. F. Kourkoutis, O. Erten, C. M. Brooks, A. S. Botana, and J. A. Mundy, *Nat. Mater.* **21**, 160 (2022).
- <sup>17</sup> Y.-T. Hsu, B. Y. Wang, M. Berben, D. Li, K. Lee, C. Duffy, T. Ottenbros, W. J. Kim, M. Osada, S. Wiedmann, H. Y. Hwang, and N. E. Hussey, *Phys. Rev. Res.* **3**, L042015 (2021).
- <sup>18</sup> Y. Cui, C. Li, Q. Li, X. Zhu, Z. Hu, Y.-f. Yang, J. Zhang, R. Yu, H.-H. Wen, and W. Yu, *Chin. Phys. Lett.* **38**, 67401 (2021).
- <sup>19</sup> M. Osada, B. Y. Wang, B. H. Goodge, K. Lee, H. Yoon, K. Sakuma, D. Li, M. Miura, L. F. Kourkoutis, and H. Y. Hwang, *Nano Lett.* **20**, 5735 (2020).
- <sup>20</sup> B.-X. Wang, H. Zheng, E. Krivyakina, O. Chmaissem, P. P. Lopes, J. W. Lynn, L. C. Gallington, Y. Ren, S. Rosenkranz, J. F. Mitchell, and D. Phelan, *Phys. Rev. Mater.* **4**, 84409 (2020).
- <sup>21</sup> S. Zeng, C. S. Tang, X. Yin, C. Li, M. Li, Z. Huang, J. Hu, W. Liu, G. J. Omar, H. Jani, Z. S. Lim, K. Han, D. Wan, P. Yang, S. J. Pennycook, A. T. S. Wee, and A. Ariando, *Phys. Rev. Lett.* **125**, 147003 (2020).
- <sup>22</sup> K. Lee, B. H. Goodge, D. Li, M. Osada, B. Y. Wang, Y. Cui, L. F. Kourkoutis, and H. Y. Hwang, *APL Mater.* **8**, 41107 (2020).
- <sup>23</sup> D. Li, B. Y. Wang, K. Lee, S. P. Harvey, M. Osada, B. H. Goodge, L. F. Kourkoutis, and H. Y. Hwang, *Phys. Rev. Lett.* **125**, 27001 (2020).
- <sup>24</sup> P. Werner and S. Hoshino, *Phys. Rev. B* **101**, 41104 (2020).
- <sup>25</sup> L. Si, W. Xiao, J. Kaufmann, J. M. Tomczak, Y. Lu, Z. Zhong, and K. Held, *Phys. Rev. Lett.* **124**, 166402 (2020).
- <sup>26</sup> F. Lechermann, *Phys. Rev. B* **101**, 81110 (2020).
- <sup>27</sup> P. Jiang, L. Si, Z. Liao, and Z. Zhong, *Phys. Rev. B* **100**, 201106 (2019).
- <sup>28</sup> H. Zhang, L. Jin, S. Wang, B. Xi, X. Shi, F. Ye, and J.-W. Mei, *Phys. Rev. Res.* **2**, 13214 (2020).
- <sup>29</sup> X. Wu, D. Di Sante, T. Schwemmer, W. Hanke, H. Y. Hwang, S. Raghu, and R. Thomale, *Phys. Rev. B* **101**, 60504 (2020).
- <sup>30</sup> M. Hepting, D. Li, C. J. Jia, H. Lu, E. Paris, Y. Tseng, X. Feng, M. Osada, E. Been, Y. Hikita, Y.-D. Chuang, Z. Hussain, K. J. Zhou, A. Nag, M. Garcia-Fernandez, M. Rossi, H. Y. Huang, D. J. Huang, Z. X. Shen, T. Schmitt, H. Y. Hwang, B. Moritz, J. Zaanen, T. P. Devereaux, and W. S. Lee, *Nat. Mater.* **19**, 381 (2020).
- <sup>31</sup> A. S. Botana and M. R. Norman, *Phys. Rev. X* **10**, 11024 (2020).
- <sup>32</sup> L.-H. Hu and C. Wu, *Phys. Rev. Res.* **1**, 032046 (2019).
- <sup>33</sup> G.-M. Zhang, Y.-f. Yang, and F.-C. Zhang, *Phys. Rev. B* **101**, 20501 (2020).
- <sup>34</sup> Y.-H. Zhang and A. Vishwanath, *Phys. Rev. Res.* **2**, 23112 (2020).
- <sup>35</sup> Y. Nomura, M. Hirayama, T. Tadano, Y. Yoshimoto, K. Nakamura, and R. Arita, *Phys. Rev. B* **100**, 205138 (2019).
- <sup>36</sup> A. Ikeda, T. Manabe, and M. Naito, *Physica C* **495**, 134 (2013).
- <sup>37</sup> M. Jiang, M. Berciu, and G. A. Sawatzky, *Phys. Rev. Lett.* **124**, 207004 (2020).
- <sup>38</sup> L.-H. Hu and C. Wu, *Phys. Rev. Res.* **1**, 032046 (2019).
- <sup>39</sup> (2019).
- <sup>40</sup> H. Sakakibara, H. Usui, K. Suzuki, T. Kotani, H. Aoki, and K. Kuroki, *Phys. Rev. Lett.* **125**, 077003 (2020).
- <sup>41</sup> J. Krishna, H. LaBollita, A. O. Fumega, V. Pardo, and A. S. Botana, *Phys. Rev. B* **102**, 224506 (2020).
- <sup>42</sup> X. Sui, J. Wang, C. Chen, X. Ding, K.-J. Zhou, C. Cao, L. Qiao, H. Lin, and B. Huang, *Phys. Rev. B* **107** (2023), 10.1103/PhysRevB.107.075159.
- <sup>43</sup> M. Kitatani, L. Si, O. Janson, R. Arita, Z. Zhong, and K. Held, *npj Quantum Mater.* **5**, 59 (2020).
- <sup>44</sup> M. Kitatani, L. Si, P. Worm, J. M. Tomczak, R. Arita, and K. Held, *Phys. Rev. Lett.* **130**, 166002 (2023), 2207.14038.
- <sup>45</sup> A. Kreisel, B. M. Andersen, A. T. Rømer, I. M. Eremin, and F. Lechermann, *Phys. Rev. Lett.* **129**, 077002 (2022).
- <sup>46</sup> C. Lu, L.-H. Hu, Y. Wang, F. Yang, and C. Wu, *Phys. Rev. B* **105**, 054516 (2022).
- <sup>47</sup> E. Pavarini, I. Dasgupta, T. Saha-Dasgupta, O. Jepsen, and O. K. Andersen, *Phys. Rev. Lett.* **87**, 047003 (2001).
- <sup>48</sup> N. Marzari, A. A. Mostofi, J. R. Yates, I. Souza, and D. Vanderbilt, *Rev. Mod. Phys.* **84**, 1419 (2012).
- <sup>49</sup> P. Blaha, K. Schwarz, F. Tran, R. Laskowski, G. K. H. Madsen, and L. D. Marks, *The Journal of Chemical Physics* **152**, 074101 (2020).
- <sup>50</sup> J. P. Perdew, K. Burke, and M. Ernzerhof, *Phys. Rev. Lett.* **77**, 3865 (1996).
- <sup>51</sup> J. E. Hirsch, *Phys. Rev. B* **28**, 4059 (1983).
- <sup>52</sup> S. R. White, D. J. Scalapino, R. L. Sugar, N. E. Bickers, and R. T. Scalettar, *Phys. Rev. B* **39**, 839 (1989).
- <sup>53</sup> R. Blankenbecler, D. J. Scalapino, and R. L. Sugar, *Phys. Rev. D* **24**, 2278 (1981).
- <sup>54</sup> T. Ma, H.-Q. Lin, and J. Hu, *Phys. Rev. Lett.* **110**, 107002 (2013).
- <sup>55</sup> T. Ma, L. Zhang, C.-C. Chang, H.-H. Hung, and R. T. Scalettar, *Phys. Rev. Lett.* **120**, 116601 (2018).
- <sup>56</sup> T. Huang, L. Zhang, and T. Ma, *Science Bulletin* **64**, 310 (2019).
- <sup>57</sup> C. Chen, R. Ma, X. Sui, Y. Liang, B. Huang, and T. Ma, *Phys. Rev. B* **106**, 195112 (2022).
- <sup>58</sup> C. Chen, Z. Fan, R. Ma, Y. Pan, Y. Liang, B. Huang, and T. Ma, *Phys. Rev. B* **109**, 045101 (2024).